J. Membrane Biol. 176, 111–117 (2000)
DOI: 10.1007/s00232001081

The Journal of
Membrane
Biology

Glycoside Binding and Translocation in Na^+-Dependent Glucose Cotransporters: Comparison of SGLT1 and SGLT3

A. Díez-Sampedro[1], M.P. Lostao[2], E.M. Wright[1], B.A. Hirayama[1]
[1]Department of Physiology, UCLA School of Medicine, 10833 Le Conte Ave., Los Angeles, California 90095-1751, USA
[2]Department of Physiology and Nutrition, University of Navarra, Pamplona, Spain

Received: 18 February 2000/Revised: 13 April 2000

Abstract. Using cotransporters as drug delivery vehicles is a topic of continuing interest. We examined glucose derivatives containing conjugated aromatic rings using two isoforms of the Na^+/glucose cotransporter: human SGLT1 (hSGLT1) and pig SGLT3 (pSGLT3, SAAT1). Our studies indicate that there is similarity between SGLT1 and SGLT3 in the overall architecture of the vestibule leading to the sugar-binding site but differences in translocation pathway interactions. Indican was transported by hSGLT1 with higher affinity ($K_{0.5}$ 0.06 mM) and 2-naphthylglucose with lower affinity ($K_{0.5}$ 0.5 mM) than α-methyl-D-glucopyranoside (αMDG, 0.2 mM). Both were poorly transported (maximal velocities, I_{max}, 14% and 8% of αMDG). Other compounds were inhibitors (K_is 1–13 mM). In pSGLT3, indican and 2-naphthylglucose were transported with higher affinity than αMDG ($K_{0.5}$s 0.9, 0.2 and 2.5 mM and relative I_{max}s of 80, 25 and 100%). Phenylglucose and arbutin were transported with higher I_{max}s (130 and 120%) and comparable $K_{0.5}$s (8 and 1 mM). Increased affinity of indican relative to αMDG suggests that nitrogen in the pyrrole ring is favorable in both transporters. Higher affinity of 2-naphthylglucose for pSGLT3 than hSGLT1 suggests more extensive hydrophobic/aromatic interaction in pSGLT3 than in hSGLT1. Our results indicate that bulky hydrophobic glucosides can be transported by hSGLT1 and pSGLT3, and discrimination between them is based on steric factors and requirements for H-bonding. This provides information for design of glycosides with potential therapeutic value.

Key words: Na^+/glucose cotransporters — *Xenopus* oocytes — Electrophysiology — Kinetics — Glucose derivatives

Correspondence to: B. Hirayama

Introduction

The Na^+/sugar cotransporters SGLT1 and SGLT3 are members of the same gene family. The amino acid identity between hSGLT1 and pSGLT3 is 66% and topology models suggest a common architecture of 14 transmembrane α-helices with several large loops (Turk & Wright, 1997). This difference in amino acid composition between SGLT1 and SGLT3 suggests that the transport functions may be different. There are differences in the substrate selectivity of SGLT1 depending on the species (Hirayama et al., 1996): for example, p-nitrophenyl-β-D-glucose, a glucose derivative with one phenyl ring, was transported by rat and human SGLT1 but it was an inhibitor of the rabbit isoform. In addition, SGLT1 transports both glucose and galactose whereas SGLT3 transports glucose but not galactose (Mackenzie et al., 1996).

Conjugation of poorly permeant compounds to glucose or galactose may help these compounds to go through the enterocyte using a Na^+/sugar cotransporter. This may improve intestinal absorption of poorly absorbable drugs (Mizuma et al., 1998). Previous studies using the rabbit SGLT1 (Lostao et al., 1994) showed that phenylglucosides can behave as transported substrates, nontransported inhibitors or noninteracting compounds depending on the nature and position of the chemical group in the phenyl ring. Adding to those results, we here provide more information about the chemical requirements for a glucose derivative to be transported. In addition, new ideas will be given about structure/function relationships because of the different affinity and transport of the compounds by both cotransporters.

Materials and Methods

Oocyte Preparation

Oocytes were obtained from adult *Xenopus laevis* as previously described (Parent et al., 1992). They were injected with 50 ng of cRNA (Ambion, Austin, TX) coding for the human Na^+/glucose cotransporter (hSGLT1, Hediger, Turk & Wright, 1989) or for the pig renal Na^+/glucose cotransporter (pSAAT1, pSGLT3, Kong, Yet & Lever, 1993; Mackenzie et al., 1994). Oocytes were maintained in Barth's medium supplemented with gentamycin (5 mg/ml), penicillin (100 units/ml)/streptomycin (100 μg/ml), at 18°C for from 3–6 days until used.

Aromatic Glycosides

All sugar conjugates were obtained from Sigma (St. Louis, MO). α-methyl-D-glucopyranoside (αMDG), phenyl-β-D-glucopyranoside (PG), 4-hydroxyphenyl-β-D-glucopyranoside (arbutin), 2-naphthyl-β-D-glucopyranoside (2-NaphGlu), phloretin-2-β-D-glucopyranoside (phlorizin, Pz), 8-hydroxyquinoline-β-D-glucopyranoside (8-HQ), 4-methylumbelliferyl-β-D-glucopyranoside (4-MU), 6,7-dihydroxycoumarin-β-D-glucopyranoside (esculin), indoxyl-β-D-glucopyranoside (indican), 1-naphthyl-β-D-galactopyranoside (1-NaphGal), and 2-naphthyl-β-D-galactopyranoside (2-NaphGal).

All other chemicals were obtained from Sigma, Research Organics (Cleveland, OH) or GibcoBRL (Gaithersburg, MD).

Electrophysiology Experiments

Experiments were performed at 22°C using the 2-electrode voltage-clamp method in a rapid perfusion chamber as previously described (Lostao et al., 1994). The membrane potential was normally held at −50 mV, but in some cases the voltage was −70 mV, and stepped for 100 msec from +50 to −150 mV in 20 mV decrements. The experiments were controlled and data acquired using pClamp software. Continuous current data was recorded using Axoscope (both from Axon Instruments, Foster City, CA).

For the transported glycosides, the steady-state sugar-dependent currents (I^s) were obtained at each voltage and glycoside concentration as the difference between the current measured at steady-state in the presence and absence of the glycoside. The apparent affinity constant ($K^s_{0.5}$) and the maximal current for saturating sugar (I^s_{max}) were obtained by fitting the steady-state currents at each membrane potential to the equation: [1] $I = I_{max} \cdot [S]/(K_{0.5} + [S])$, using the nonlinear fitting method in SigmaPlot (SPSS, Chicago, IL) where [S] is the glycoside concentration. It was previously shown for SGLT1 that the apparent affinity, $K_{0.5}$, is a fair approximation for the binding affinity (k_{23}/k_{32}) (Parent et al., 1992).

For inhibitors the apparent inhibition constant (K_i) was determined at each membrane potential by measuring the difference between the αMDG current in the presence of the blocker and in its absence. These values were fit to Eq. [1] where I is the sugar-dependent current inhibited by the glycoside and [S] is the inhibitor concentration. [αMDG] was 0.4 mM for hSGLT1 and 4.0 mM for pSGLT3.

Results

The type of interaction of the glucose- and galactose-conjugates was initially determined by measuring the current generated in transporter-expressing oocytes. Figure 1 shows an example of a continuous current record using hSGLT1 voltage-clamped to −50 mV. Initially the oocyte was bathed in a 100 mM NaCl buffer, and when 1 mM αMDG was added to the bath an inward current was generated over baseline by −870 nA. This is the result of sugar: Na^+ cotransport in which 2 Na^+ ions are cotransported simultaneously with one sugar, generating a current of positive charge into the oocyte (Mackenzie, Loo & Wright, 1998). Indican (2 mM) also induced an inward current (20% of the αMDG transport, 200 *vs.* 870 nA) indicating that it (as well as 2-NaphGlu, *not shown*), was a transportable substrate. In contrast, esculin (10 mM) had no apparent effect on the current, but this compound was an inhibitor of Na^+/sugar cotransport. 10 mM esculin inhibited the 1 mM αMDG current by ~25%. 7 mM 1-NaphGal, 7 mM 2-NaphGal, 20 mM 8-HQ and 10 mM 4-MU showed the same behavior as esculin: inhibition of 1 mM αMDG current but neither inward current nor inhibition of the baseline current. Phlorizin, the characteristic competitive inhibitor of Na^+/glucose cotransporters (Toggenburger et al., 1982) reduced the

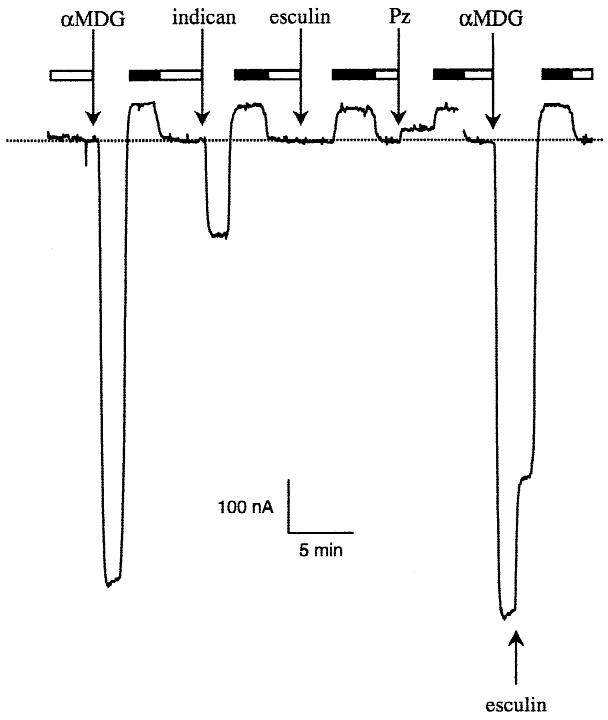

Fig. 1. Na^+ current was measured in a single hSGLT1 injected oocyte in the presence of different glycosides. The membrane potential was clamped at −50 mV. The dotted horizontal line indicates the baseline current in Na^+ medium in the absence of substrate. The addition of 1 mM αMDG and 2 mM indican induced inward currents, 100 mM Pz reduced the baseline current and 10 mM Esculin did not produce a current but inhibited the αMDG current by 30%. After the addition of each sugar, the oocyte was washed out in Na^+-free medium (black box) followed by Na^+ medium (blank box).

baseline current, a consequence of its inhibition of the sugar-uncoupled 'leak' current of Na^+ through hSGLT1 (Umbach, Coady & Wright, 1990). Similar experiments with pSGLT3 also showed that indican and 2-NaphGlu were transported, 4-MU and 8-HQ were inhibitors, and esculin and the Naphthyl-galactosides did not significantly interact with pSGLT3 (Table).

Kinetics studies were then performed to obtain the apparent affinities ($K_{0.5}$) and maximal currents (I_{max}). Figure 2 (upper panel) shows αMDG and indican Na^+ inward currents at different concentrations, from 0.01 to 2 mM, in a single hSGLT1-expressing oocyte clamped at −70 mV. Apparent affinity (Eq. [1]) values were not voltage sensitive between −150 and −10 mV. These results indicated a 5-fold higher affinity of indican ($K_{0.5}$) for hSGLT1 but a 7-fold lower maximal current than αMDG. In pSGLT3 (lower plot) the $K_{0.5}$s and I_{max}s for both compounds were comparable.

In addition, kinetics for phenyl-β-D-glucose and arbutin were measured in hSGLT1 and pSGLT3. Both hSGLT1 and pSGLT3 identified the same compounds as transported substrates, but the nature of the interactions were different, for example, phenyl-β-D-glucose, a poor affinity substrate of both hSGLT1 and pSGLT3 (1.6 and 7.9 mM) was poorly transported in hSGLT1 (25% of αMDG I_{max}) but well transported in pSGLT3 (130% of αMDG I_{max}). Kinetic parameters for transport including 2-NaphGlu, and arbutin are summarized in the Table.

Apparent inhibition constants (K_i) were estimated for sugar analogues by determining the concentration dependence of inhibition of the αMDG-dependent close to the $K_{0.5}$ for each transporter. Figure 3 shows that for 8-hydroxyquinoline-β-D-glucoside the K_i for hSGLT1 was 6 mM, but the affinity of pSGLT3 was very low, so at the highest concentration (20 mM) only 25% of the αMDG current was inhibited, suggesting a K_i of ~40 mM. The order of affinities (highest affinity to lowest) in hSGLT1 was Pz >> 1-NaphGal > 8-HQ ≥ 4-MU ≥ 2-naphGal > esculin (*see* Table). In pSGLT3 the order was Pz >> 4-MU > 8-HQ (Table), with no interaction of esculin or the two galactosides.

Discussion

The two transporters hSGLT1 and pSGLT3 are homologous and share a common architecture, but their functional details are different. We can obtain information about the binding and cotransport mechanisms by comparing how these transporters interact (affinity and translocation) with a set of glycosides. In this study we only used β-linked glycosides and galactosides because it has been demonstrated that, while SGLT3 transports bulky α-linked glucosides, SGLT1 does not (Lostao et al., 1994; Mackenzie et al., 1996).

The compounds transported by hSGLT1 were also mostly transported by pSGLT3, and both of the Na^+-dependent glucose cotransporters are capable of transporting glycosides at least as large as 2-naphthyl-β-D-glucose (estimated maximum dimensions 11Å × 5Å × 4Å). Some of these compounds have apparent affinities higher than that for the model sugar αMDG. Additions to the aromatic rings decreased affinity in both transporters.

Affinity for Glucosides

In hSGLT1 the affinity (we will stipulate that our usage of 'affinity' is actually the apparent affinity for transport or inhibition) for the transported glycosides increased in the order: esculin < 4-MU < 8-HQ < PG < arbutin < 2-NaphGlu < αMDG < glucose < indican < phlorizin (Table). SGLT1 behaves as if it has a hydrophobic/aromatic region in the vestibule in the vicinity of binding site Carbon 1 (C1) of the pyranose ring, however the size and details of its architecture remain to be established. This feature is the reason that attaching an aromatic ring via a β-linkage can create a transported substrate, whereas disaccharides are ignored and α-linked glucosides are poorly recognized (Landau, Bernstein & Wilson, 1962; Mizuma, Ohta & Awazu, 1994; Lostao et al., 1994). The high affinity of indican and 2-naphthylglucose, compared to αMDG and the inhibitors 4-MU, 6-HQ and esculin, suggests a model in which a significant portion of binding strength is derived from hydrophobic interactions, whereas discrimination of an acceptable structure *vs.* ones that will not bind, is determined by the H-bonding interactions between the vestibule and groups decorating the aromatic rings and steric interactions. In rabbit SGLT1, the affinity and transportability of phenyl glucose increased with the addition of a −OH in the *para*-position (factor of 3 for $K_{0.5}$ and 1.5 for I_{max}), and we have previously shown that the *ortho*-position accommodates H-bond acceptors but not donors (Lostao et al., 1994). In hSGLT1, the addition of a *para*-OH did not affect affinity but increased the I_{max}. This process of substrate identification bears striking similarity to that of the sugar-transporting porins (reviewed by Jap and Walian (1998)).

In pSGLT3 the affinity for the same set of glycosides increased in the order: 8-HQ < 4-MU < PG < glucose < αMDG < arbutin < indican < 2-NaphGlu < phlorizin (Esculin did not interact with SGLT3) (Table). As in SGLT1, it appears to be a hydrophobic/aromatic surface outside of the sugar binding site which interacts with β-linked aromatic rings and a capacity for H-bonding that increased the affinity for arbutin (1.2 mM) compared to PG (7.9 mM). Increasing the size of the aromatic moiety to indican and 2-NaphthylGlu, resulted in a further increase in affinity ($K_{0.5}$ = 0.9 and 0.2 mM), suggesting that the larger aromatic systems were

Table. Summary of glycoside kinetics in hSGLT1 and pSGLT3

	hSGLT1				pSGLT3	
A	I_{max}(%)	K_m (mM)	Compound	Structure	I_{max}(%)	K_m (mM)
	100	$0.2_{(2,4)}$	D-Glucose	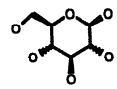	100	$6_{(3)}$
	100	$0.2_{(2)}$	D-Galactose	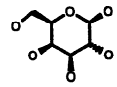	–	$>>20_{(3)}$
	100	$0.3_{(1,2)}$	α-Methyl-D-glucose	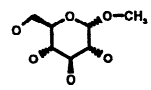	100	$2.5_{(3,4)}$
	90	$3.3_{(1)}$	3-O-Methyl-glucose	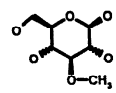	ND	$NI_{(3,4)}$
	8	0.5 ± 0.2	2-Naphthyl-β-D-glucose	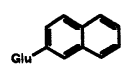	25 ± 3	0.2 ± 0.01
	14	0.06 ± 0.01	Indican	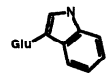	80	0.9 ± 0.2
	25	1.6 ± 0.2	Phenyl-β-D-glucose		130	7.9 ± 0.5
	74	1.3 ± 0.2	Arbutin	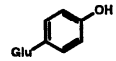	120	1.2 ± 0.1
B		K_i (mM)	Compound	Structure		K_i (mM)
	–	$0.00022_{(1)}$	Phlorizin	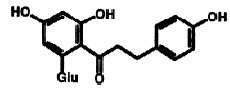	–	$0.009_{(3)}$
	–	9 ± 3	4-Methylumbelliferyl-β-D-glucose	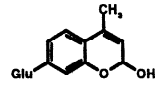	–	3.3 ± 1
	–	6 ± 2	8-Hydroxyquinoline-β-D-glucose	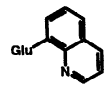	–	~40
	–	13 ± 4	Esculin	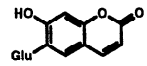	–	NI
	–	1 ± 0.3	1-Naphthyl-β-D-galactose	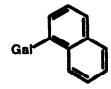	–	NI
	–	10 ± 2	2-Naphthyl-β-D-galactose	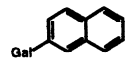	–	NI

(*A*) Glycosides transported. (*B*) Glycosides nontransported (note that galactose is not transported by SGLT3). The data from this study are combined with data obtained with similar methods in previous studies (references in subscripts). Note that phlorizin affinity is reported as a K_i. Kinetics are mean ± SEM from at least 3 oocytes from at least 2 different donor frogs. ND = not determined; NI = no consistent significant effect at maximum solubility of test glycoside. (Mackenzie et al. 1994; Hirayama et al., 1996; Mackenzie et al., 1996; Hirayama et al. 1997).

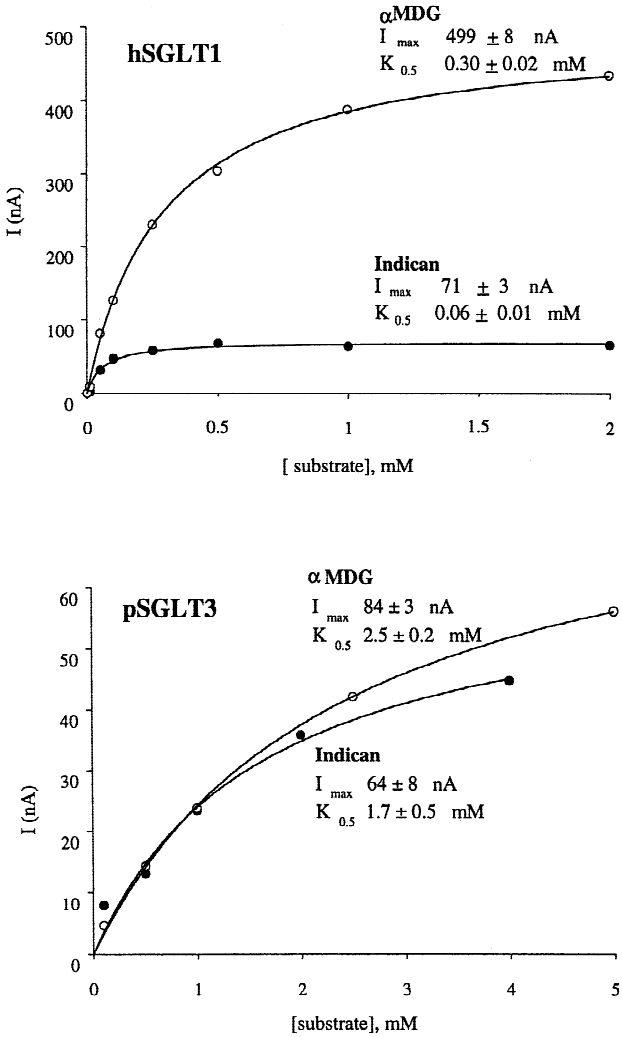

Fig. 2. Kinetics of indican on hSGLT1 and pSGLT3 at a membrane potential of −70 mV. An example of the dependence of the Na^+ inward currents on αMDG and indican concentration in hSGLT1- (upper panel) and pSGLT3-injected (lower panel) oocytes. Kinetic constants were obtained according to experimental procedures. Similar results were obtained with oocytes from different frogs. The results are summarized in the Table. (The maximal currents recorded are a function of protein expression levels, which depend on the batch of oocytes and the individual clone; the turnover number for hSGLT1 and pSGLT3 are both ~50 sec^{-1} at −150 mV, *unpublished results.*)

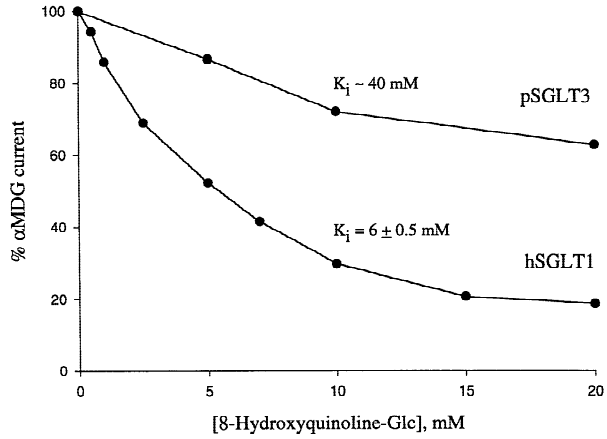

Fig. 3. Apparent inhibition constant (K_i) of 8-HQ for hSGLT1 and pSGLT3. The αMDG current inhibited was determined for each concentration of 8-HQ, and the inhibition constant was estimated by fitting the data to Eq. [1].

stabilized in the binding site. The 2-fold increase in affinity for αMDG ($K_{0.5}$ = 2.5 mM) over glucose ($K_{0.5}$ = 6 mM) may also be a reflection of an increase in stability in the binding site due to hydrophobic interactions of the methyl group with the vestibule. Increasing the number of −OH, =O, or $-CH_3$ groups to the 2-naphthyl ring (4-MU and esculin) reduced affinity. This may be due to incompatible H-bonding requirements, steric effects in the vestibule or, particularly in the case of esculin, conformational restrictions due to the proximity of the −OH group to glucose (Table).

The highest affinity inhibitor was phlorizin for both transporters, with affinities from 600–1,000 times that of glucose. The phlorizin affinity of SGLT1 is 40 times higher (K_i = 0.22 μM, Hirayama et al., 1996) than that of SGLT3 (K_i = 9 μM, Mackenzie et al., 1996). This is similar to the ratio of affinities for glucose in the two transporters (SGLT1:SGLT3 = 30:1). We note that the characterization of phlorizin, or other compounds, as an inhibitor is an operational definition. Previous studies suggest that phlorizin may be transported at a very low rate by SGLT1 (Lostao et al., 1994), and Panayotova-Heiermann et al. (1996) described a SGLT1-SGLT3 chimeric transporter in which phlorizin was the highest affinity transported substrate.

SGLT1 has a higher affinity for sugar than SGLT3, however the SGLT3 sugar-binding site is more selective. The $K_{0.5}$ of SGLT1 for αMDG, for example, is ~0.3 mM, compared to ~2.5 mM for SGLT3, however SGLT3 does not bind or transport galactose or 3-O-methylglucose (Table). What do these differences tell us about how sugar conjugates bind to the transporter? The lack of interaction of the naphthylgalactosides with pSGLT3 indicates that the primary discrimination for sugar conjugates is the sugar-binding site. 2-naphthylglucose showed a 30-fold increase in apparent affinity compared to glucose. This indicates that binding of the naphthyl moiety in the vestibule lowered the free energy of the system. 2-Naphthylgalactose, however, was ignored by pSGLT3, and this indicates that the contribution by the naphthyl group to binding energy was insignificant compared to the discrimination against the galactose moiety. Interestingly, the 1-naphGal and 2-naphGal were inhibitors of hSGLT1, and the affinity of 2-naphGal was 20-fold lower than the glucoside (Table). The reason for this discrepancy is not yet understood, but it is possible that the orientation of glucose in the binding site

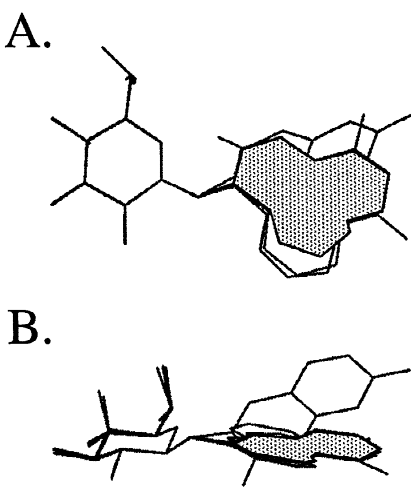

Fig. 4. Conformational searches about the glycosidic bond of all of the compounds used in this study. After the initial structures were relaxed, charges were assigned to the atoms using the AM1 semi-empirical method, and the final structures were determined using the MM+ forcefield (Hyperchem, Hypercube, Ontario, Canada) using these atomic charges. The 7 lowest energy structures were compared with the crystal structures of 4-methylumbelliferyl-β-D-glucopyranoside (GEMDOR) and salicin (CIZWOX) deposited in the Cambridge Structural Database. As the differences in energy between the different conformations was small, we compared the structures which had torsions closest to that of the first ring of 4-MU. The structures were superimposed on the pyranose ring oxygen 5, carbon 1 and oxygen 1.

is slightly different from that of galactose to accommodate the different configuration of the −OH at C4, and this results in a greater degree of incompatibility in the vestibule, which is reflected in a lower apparent affinity.

The Fig. 4 compares the 3-D structures of the test compounds. The aromatic rings of the transported substrates (arbutin, indican and 2-naphthyl-glucose) are shaded. Panel *A* shows that the area of the aromatic rings or substituent groups of the nontransported compounds extend beyond the boundaries defined by indican and 2-NaphGlu, suggesting a size limit for transport of approximately 5Å × 4Å. Panel *B* is a side view of the overlay. All of the aromatic rings are predicted to lie in the same plane, except esculin, which projects out of the plane by ~30°. This may account for the lower affinity of hSGLT1 for esculin binding because the aromatic surface is not in contact with the vestibule. The lack of interaction with pSGLT3 may be the result of a steric conflict preventing binding of the glucose moiety.

Translocation of the Sugar

It has been previously shown for rabbit SGLT1 that maximal transport velocity (I_{max}) is not correlated to the affinity for either the underivatized transported sugars (Birnir, Loo & Wright, 1991), or the aromatic glucosides (Lostao et al., 1994). Adding a *para*-OH to PG (arbutin) increased the I_{max} by 50%, suggesting that the translocation through the protein also involved H-bonding. The same characteristics were observed for hSGLT1, where the I_{max} increased in the order: 2-NaphGlu < indican < PG < arbutin < glucose, αMDG (Table). Increasing the number of functional groups on 2-NaphGlu allowed binding but turned the compound into an inhibitor, suggesting that the placement of the groups was incompatible with the translocation pathway.

There appears to be differences in the translocation pathway between hSGLT1 and pSGLT3. (i) All the simple sugars that SGLT3 transports have the same I_{max}, but the Table shows that addition of an aromatic ring increased the I_{max} of the PG conjugate to 130% of the I_{max} for αMDG. Addition of a *para*-OH had no significant effect on I_{max} (or affinity). (ii) Increasing the size of the conjugate reduced turnover rate, so for pSGLT3 I_{max} for indican was 80% of I_{max} for αMDG, whereas I_{max} for 2-NaphthylGlu was 25% suggesting that the pyrrole nitrogen in the first aromatic ring is involved in a favorable interaction in the translocation pathway. In hSGLT1 the effects on I_{max} were much more dramatic, decreasing to 14 and 8% of I_{max} for αMDG. pSGLT3 did not tolerate additional functional groups on 2-NaphGlu or the influence of nitrogen in the second aromatic ring of 8-HQ.

Several groups have investigated the possibilities of using SGLT1 and SGLT3 as drug delivery vehicles. Recent studies demonstrated transport of acetaminophen-glucose by rat SGLT1 (Mizuma et al., 1998) and ifosfamide mustard-glucoside by SGLT3 (Vehyl et al., 1998). We would expect that acetaminophen-β-D-glucose would bind to SGLT1 because of the favorable placement of the aromatic ring on C1, and the *para*-placement of the nitrogen serves a similar H-binding role as the para-OH of arbutin. The carbonyl and aliphatic portions are compatible with the requirements for aromatic and hydrophobic interactions in this region. The similarity in requirements for transport by SGLT3 also suggest that acetaminophen-glucoside should be a good substrate. On the other hand, ifosfamide mustard-glucoside was well transported by SGLT3 (K_m = 1.1 mM, and V_{max} ~5-fold lower than αMDG, Vehyl et al., 1998) but was not transported by human or rabbit SGLT1. Our data suggest that the charged/polar nature of the phosphate is incompatible with the hydrophobic region of the vestibule. Future interactions with SGLT3 will provide further information on the characteristics of the binding transport pathway.

What steps in the transport process account for these effects on transport? According to our 6-state alternating access model of cotransport (Parent et al., 1992; Loo et al., 1998; Loo et al., 2000) the affected rate constants are confined to substrate binding/release or translocation of

the fully loaded transporter. (The ion-binding and translocation of the empty transporter are unaffected.) This is because the ion-driven cotransporters behave as if at least one cation binds first, inducing a conformational change in the protein at the sugar binding site, the result of which is to increase affinity for sugar. Binding of sugar in turn induces a conformational change that results in reorientation of the binding sites to now face the interior of the cell, where the substrates are released. At this point it is not possible to differentiate between these steps. So, for example, for a nontransported compound that binds to the transporter, the defect could be in either the translocation of substrate release steps. Our continuing studies are investigating in detail how these compounds affect the transporter by exploiting the biophysical characteristics of SGLT1.

We thank Daisy Leung and Mary L. Bing for the isolation and preparation of the oocytes, Dr. Maria Font for discussions on the chemistry of the compounds. This work was supported by National Institutes of Health Grants NIH 19567, DK 44602 and GM 52094 and by PIUNA of the University of Navarra in Spain.

References

Birnir, B., Loo, D.D.F., Wright, E.M. 1991. Voltage-clamp studies of the Na^+/glucose cotransporter cloned from rabbit small intestine. *Pfluegers Arch.* **419:**79–85

Hediger, M.A., Turk, E., Wright, E.M. 1989. Homology of the human intestinal Na^+/glucose and *Escherichia coli* Na^+/proline cotransporters. *Proc. Natl. Acad. Sci. USA* **86:**5748–5752

Hirayama, B.A., Loo, D.D.F., Wright, E.M. 1997. Cation effects on protein conformation and transport in the Na^+/glucose cotransporter. *J. Biol. Chem.* **272:**2110–2115

Hirayama, B.A., Lostao, M.P., Panayotova-Heiermann, M., Loo, D.D.F., Wright, E.M. 1996. Kinetic and specificity differences between rat, human, and rabbit Na^+-glucose transporters (SGLT-1). *Am. J. Physiol.* **270:**G919–G926

Jap, B.K., Walian, P.J. 1998. Gliding through sugar channels: how sweet it is! *Nat. Struct. Biol.* **5:**6–8

Kong, C.T., Yet, S.F., Lever, J.E. 1993. Cloning and expression of a mammalian Na^+/amino acid cotransporter with sequence similarity to Na^+/glucose cotransporters. *J. Biol. Chem.* **268:**1509–1512

Landau, B.R., Bernstein, L., Wilson, T.H. 1962. Hexose transport by hamster intestine in vitro. *Am. J. Physiol.* **230:**237–240

Loo, D.D.F., Eskandari, S., Hirayama, B.A., Wright, E.M. 2000. A kinetic model for secondary active transport. (*in press*)

Loo, D.D.F., Hirayama, B.A., Gallardo, E.M., Lam, J.T., Turk, E., Wright, E.M. 1998. Conformational changes couple Na^+ and glucose transport. *Proc. Natl. Acad. Sci. USA* **95:**7789–7794

Lostao, M.P., Hirayama, B.A., Loo, D.D.F., Wright, E.M. 1994. Phenylglucosides and the Na^+/glucose cotransporter (SGLT1): Analysis of interactions. *J. Membrane Biol.* **142:**161–170

Mackenzie, B., Loo, D.D.F., Panayotova-Heiermann, M., Wright, E.M. 1996. Biophysical characteristics of the pig kidney Na^+/glucose cotransporter SGLT2 reveal a common mechanism for SGLT1 and SGLT2. *J. Biol. Chem.* **271:**32678–32683

Mackenzie, B., Loo, D.D.F., Wright, E.M. 1998. Relationship between Na^+/glucose cotransporter (SGLT1) currents and fluxes. *J. Membrane Biol.* **162:**101–106

Mackenzie, B., Panayotova-Heiermann, M., Loo, D.D.F., Lever, J.E., Wright, E.M. 1994. SAAT1 is a low affinity Na^+/Glucose cotransporter and not an amino acid transporter. A reinterpretation. *J. Biol. Chem.* **269:**22488–22491

Mizuma, T., Nagmine, Y., Dobashi, A., Awazu, S. 1998. Factors that cause the β-anomeric preference of Na^+/glucose cotransporter for intestinal transport of monosaccharide conjugates. *Biochim. Biophys. Acta* **1381:**340–346

Mizuma, T., Ohta, K., Awazu, S. 1994. The beta-anomeric and glucose preferences of glucose transport carrier for intestinal active absorption of monosaccharide conjugates. *Biochim. Biophys. Acta* **1200:** 117–122

Panayotova-Heiermann, M., Loo, D.D.F., Kong, C.T., Lever, J.E., Wright, E.M. 1996. Sugar binding to Na^+/glucose cotransporters is determined by the carboxyl-terminal half of the protein. *J. Biol. Chem.* **271:**10029–10034

Parent, L., Supplisson, S., Loo, D.D.F., Wright, E.M. 1992. Electrogenic properties of the cloned Na^+/glucose cotransporter: II. Transport model under nonrapid equilibrium. *Biophys. J.* **59:**63–79

Toggenburger, G., Kessler, M., Semenza, G., 1982. Phlorizin as a probe of the small intestinal Na^+, D-glucose cotransporter. A model. *Biochim. Biophys. Acta* **688:**557–571

Turk, E., Wright, E.M. 1997. Membrane topology motifs in the SGLT cotransporter family. *J. Membrane Biol.* **159:**1–20

Umbach, J.A., Coady, M.J., Wright, E.M. 1990. Intestinal Na^+/glucose cotransporter expressed in *Xenopus* oocytes is electrogenic. *Biophys. J.* **57:**1217–1224

Veyhl, M., Wagner, K., Volk, C., Gorboulev, V., Baumgartner, K., Weber, W.M., Schaper, M., Bertram, B., Wiessler, M., Koepsell, H. 1998. Transport of the new chemotherapeutic agent β-D-glucosylphosphoramide mustard (D-19575) into tumor cells is mediated by the Na^+-D-glucose cotransporter SAAT1. *Proc. Natl. Acad. Sci. USA* **95:**2914–2919